

Theoretical Study of Isotope Fractionation Effects in Different Systems Based on First Principles

Renxue Shi¹, Jiajia Lu¹, Pingjiao Xie¹ & Lanlan Wu¹

¹ School of Karst Science, Guizhou Normal University, Guiyang, China; State Engineering Technology Institute for Karst Desertification Control, Guizhou Normal University, Guiyang, China

Correspondence: Renxue Shi, School of Karst Science, Guizhou Normal University, Guiyang, China; State Engineering Technology Institute for Karst Desertification Control, Guizhou Normal University, Guiyang, China.

Received: May 8, 2025 Accepted: June 6, 2025 Online Published: June 10, 2025

Abstract

The study of theoretical calculation work of isotope fractionation effect provides a good theoretical basis for the research of geochemistry and other related disciplines. Numerous scholars use different calculation methods which may lead to the deviation of the calculation results. In this work, we calculated some gases, liquids, and minerals systems by Gaussian software with two different methods, B3LYP/6-311+G(d, p) and HF/3-21G. Theoretical calculation results could be compared with the previous experimental and natural sample measurements in this field. The comparison between theoretical calculation and experimental results could come up with which theoretical method is closer to the results of many kinds of research, and provide a direction for future researchers when choosing to apply the theoretical methods. This study draws some preliminary conclusions as follows: 1. The isotope fractionation effect of isotopologue with light atoms is greater than that with heavy atoms. 2. The isotope fractionation factors are a function of temperature, and these parameters decrease with the temperature increase. 3. The calculations with the HF/3-21G method are not very accurate. The calculations with the B3LYP/6-311+G(d, p) method are closer to the results of many research works than those of the HF/3-21G method.

Keywords: isotope fractionation, theoretical calculations, B3LYP/6-311+G(d, p), HF/3-21G

1. Introduction

The isotope fractionation factors are used to assess and quantify the difference in isotope distribution between different substances or two phases. Theoretical calculations deepen our comprehension of isotope distribution and migration patterns within both natural and anthropogenic geochemical processes, which is crucial for the fields of earth sciences, environmental sciences, and related disciplines. Methods of calculating isotope fractionation factors include experimental determination, measurement of natural samples, and theoretical calculation. The experiment method is an important technological means to obtain data. Measurement of natural samples usually involves analyzing the distribution of isotopes in natural samples and estimating the isotope fractionation factor. The difficulty of this method is that it needs to accurately grasp whether the sample has reached isotope equilibrium[1]. Theoretical calculations based on statistical mechanics and quantum mechanics principles, predict fractionation factors by calculating the partition function ratios of reactants and products of an isotope exchange reaction. In the traditional measurement of isotope fractionation factors, researchers often obtain data by analyzing natural samples and experiments. However, the specific microscopic processes of these chemical reactions are not quite understood. Examining the basic theory of stable isotope fractionation can help explain and analyze the experimental process and its measurement data of natural samples. Theoretical calculation could offer a unique perspective to help find the root cause of fractionation[2]. Besides, understanding this theory becomes particularly powerful in systems that are difficult to characterize experimentally or for which empirical data are scarce. It has important implications for understanding experimental processes[3].

The theory of stable isotope fractionation originated in 1919 when Lindemann and co-authors used statistical thermodynamics to calculate vapor pressure differences between lead isotopes[4]. In 1935, Urey and Greiff made an early study of stable isotope fractionation theory by exchanging isotopes of hydrogen, lithium, carbon, nitrogen, oxygen, and halogens between various diatomic and polyatomic molecules [5]. Urey explained isotope fractionation calculations through vibrational zero-point energies, ultimately simplifying the equations for determining molecular isotope partition function ratios[6]. This foundational work in stable isotope geochemistry

is known as the Urey model or Bigeleisen-Mayer formula in the geochemical community [7]. In the foundational studies by Urey and Bigeleisen, systematic calculations were conducted for parameters of simple gas molecules. In subsequent studies, the theoretical calculations were oriented to different fields and objects. The most classical of the theoretical calculations for gases is the large compilation by Richet et al. of the traditional isotope systems of C, H, O, N, S, and Cl [8]. Adnew et al.'s work updated Richet's data by examining the temperature dependence of oxygen isotope fractionation factors[9]. In condensed matter, Bigeleisen documented the influence of molecular structure on isotope differences in thermodynamic properties for liquid and solid states [10]. Jakli et al. measured the effects of vapor pressure for NaBr, NaI, KF, Na₂SO₄, and CaCl₂ in water and hydrated crystals [11]. Bottiga applied theoretical calculations to fluids, evaluating fractionation factors for carbon and oxygen isotopes in calcite-carbon dioxide-water systems[12]. Many other researchers have used this method in some crystals and their amorphous solids. Zheng, for example, studied oxygen isotope fractionation between quartz, dolomite, and water, as well as between metal oxides[13]. Xiao et al. utilized density functional theory to investigate calcium isotope fractionation in potassium carbonates, selenium carbonates, sphalerite, and calcium-bearing minerals [14]. Ferrari et al. calculated equilibrium isotope fractionation factors for antimony in antimony-bearing minerals, noting that secondary antimony minerals exhibit heavier isotopic signatures than primary gabbro ores [15]. Duan et al. investigated Mg isotope fractionation in mantle minerals, finding that variations in cation sites can result in significant differences in Mg isotope equilibrium between minerals, indicating that site-specific effects are common in solid materials [16]. Stable isotope fractionation theory also has applications in conventional light isotope systems. Criss et al. calculated the temperature dependence of isotope fractionation factors and described the distribution principles [17]. With the improvement of isotope analysis techniques, the elemental set of natural isotopes that can be detected has expanded. For instance, Yang et al. analyzed cadmium isotope fractionation in hot solutions, while Zhao et al. studied cadmium fractionation during complexation with organic ligands[18-19]. Further studies on cadmium isotopes have been conducted by Komárek et al. and Ratié et al. [20-21]. Theoretical and experimental research has similarly explored isotope fractionation for metals such as lithium, iron, magnesium, strontium, and vanadium[22-26].

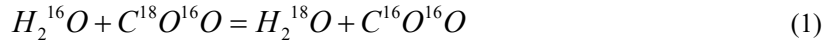
First-principles quantum chemistry calculations encompass various computational methods, including semi-empirical methods primarily applied to large organic molecular systems but generally unsuitable for metal-bearing systems. Common semi-empirical methods include AM1, PM3, CNDO, and MINDO, etc. The commonly used ab initio methods are HF, RHF, UHF, ROHF, etc. These ab initio methods represent the most basic level of such calculations and are generally unsuitable for energy calculations beyond structure optimization. Density-functional methods, such as B3LYP, MO6, and WB97XD, are the most widely used [27-29]. Nowadays, there are also various chemical software applied to theoretical calculations, commonly used are Quantum Espresso[30-31], Gaussian 16[32], VASP [33] and so on. Compared to other software, Gaussian software is easy to start and has strong integration. Structure optimization, frequency calculation, transition state finding, NMR spectroscopy, and ICR can be done with this software. There is a graphical interface that is easy to start, and suitable for researchers in various fields. Therefore, many researchers choose to use this software. In Gaussian software, the calculation methods include HF, B3LYP, PBE|PBE, PKZB, TPSS, and so on. The basis groups are all-electronic basis sets such as sto-3g, 3-21g, 6-31g, d95v, etc. which are usually coupled with polarization functions (adding “**” “***” etc., to the standard basis sets) and dispersion functions (adding “+” or “++”) are used. The pseudopotential basis sets LANL1MD, LANL2MD, LANL2DZ, CEP-4G, SDD, etc., are usually suitable for heavy-element basis groups. There are also the hybrid basis groups GEN and PSEUDO=READ, etc. In this paper, several elements such as C, H, O, N, S, and Cl are studied based on Urey-Model (or Bigeleisen-Mayer equation). GaussView6.0 and Gaussian16 software were used to construct the gaseous molecule structures and calculate simple harmonic vibration frequencies. The commonly used two methods for Gaussian software are B3LYP/6-311+G(d, p) and HF/3-21G. The isotope fractionation factors between different gaseous molecules were calculated by analyzing and comparing the values of different intermolecular reduced partition function ratios (RPFR). The fractionation values varied for different elemental forms, and these results were compared with previous studies to assess the differences among calculation methods. And the results can provide a reference value for researchers when choosing calculation methods.

2. Theory and Research Methodology

2.1 Research Theory

The method we used is the formula proposed by Bigeleisen and Mayer in 1947, known as the Bigeleisen-Mayer formula (also called the Urey model)[6-7]. The model relates the chemical equilibrium constant K to the isotope fractionation factors commonly used in geochemistry and yields a formula that allows K to be derived by simple harmonic vibrational frequencies. In other words, isotope fractionation factors can be obtained at the molecular

level through basic theoretical simulations and calculations. Take the isotope exchange reaction between water and carbon dioxide molecules in this paper as an example:



Where “16” and “18” are two different isotopes of oxygen. According to the statistical thermodynamic theory, the isotope fractionation factor α of the above isotope exchange reaction is:

$$\alpha_{H_2O-CO_2} = K^{\frac{1}{n}} \quad (2)$$

In Eq. 2, “ K ” is the chemical equilibrium constant of the reaction, and “ n ” is the number of atoms exchanged in the isotope exchange reaction. In all the studies of this paper, only one atom is exchanged in the isotope exchange reactions, i.e., α is equal to K . The equilibrium constant, K , can be expressed in terms of the reduced partition function ratio:

$$K = \frac{RPFR(H_2O)}{RPFR(CO_2)} \quad (3)$$

The theoretical formula for RPFR (reduced partition function ratio) can be obtained from the Bigeleisen-Mayer formula as

$$RPFR = \left(\frac{s^{18}}{s^{16}} \right)^{3n-6} \prod_i \frac{u_i^{16}}{u_i^{18}} \frac{\exp(-u_i^{16}/2)}{\exp(-u_i^{18}/2)} \frac{1 - \exp(-u_i^{18})}{1 - \exp(-u_i^{16})} \quad (4)$$

The “ s ” in Eq. 4 is the symmetrical number of the object under study, which is constant before and after the isotope exchange reaction for most reactions. “ u_i ” is a function of the simple harmonic vibrational frequencies:

$$u_i = \frac{hv_i}{kT} \quad (5)$$

“ v_i ” represents the simple harmonic vibrational frequency of the molecule, “ k ” and “ h ” are Boltzmann’s and Planck’s constants, respectively, and “ T ” is the Kelvin temperature. Thus, there is only one variable “ v_i ”. i.e., we can obtain the isotope fractionation factor of a substance at any temperature by requiring only the simple harmonic vibrational frequencies of the molecule. The isotope fractionation factor between any two phases of a substance can be calculated from the additivity between isotope effects, i.e.:

$$10^3 \ln \alpha_{H_2O-CO_2} = 10^3 \ln RPFR_{H_2O} - 10^3 \ln RPFR_{CO_2} \quad (6)$$

Or it is expressed as:

$$\alpha_{H_2O-CO_2} = \frac{RPFR_{H_2O}}{RPFR_{CO_2}} \quad (7)$$

2.2 Solid Mineral Modeling

We used the volume variable cluster method (VVCM) to calculate minerals. This method has been used in many different geological systems with good results [33-36]. Before modeling, we first enter the crystal database. In this study, we enter the ruff crystal database to find the molecular model of the object to be studied, i.e., calcite and dolomite[37]. For minerals, the basic unit that represents the structure of the mineral is the crystal cell. Given that the isotope effect is a local property, a representative partial fragment is clipped, and the target atom is positioned at the center of the mineral fragment. To maintain electroneutrality, virtual charges were added to neutralize the remaining electrons in the mineral fragments, ensuring a realistic chemical environment. The distances between these virtual charges and the outermost atoms were adjusted continually to achieve the most stable, lowest-energy structure. Figure 1 shows the molecular cluster models of dolomite and calcite built in this study, where "a" and "b" represent calcite and dolomite, respectively.

2.3 Simulation of Solvation Effect

The “water droplet method” based on the molecular cluster model was used to construct the solution model. The interested atom is placed in the center and water molecules are gradually added around it to make the model look

like a small droplet [38]. i.e., the atoms of interest are surrounded by water molecules. For example, in the sulfate solution in this study (Figure. 2), sulfate is placed in the center and six water molecules are added around it to form an octahedral structure. The water molecules added for the first time are called the first coordination layer, and then another six water molecules are added around the model, i.e., the second coordination layer. Structural optimization and frequency calculations through Gaussian software used the same theoretical base level for these two processes. Based on previous experience, the water molecules of the sixth layer have minimal impact on the isotope effect of the central atom. Therefore, the process can be considered complete when the sixth layer of water molecules is added. To enhance reliability, four parallel calculations were conducted for structure optimization and frequency calculations, and the arithmetic mean of these calculations was taken as the final results.

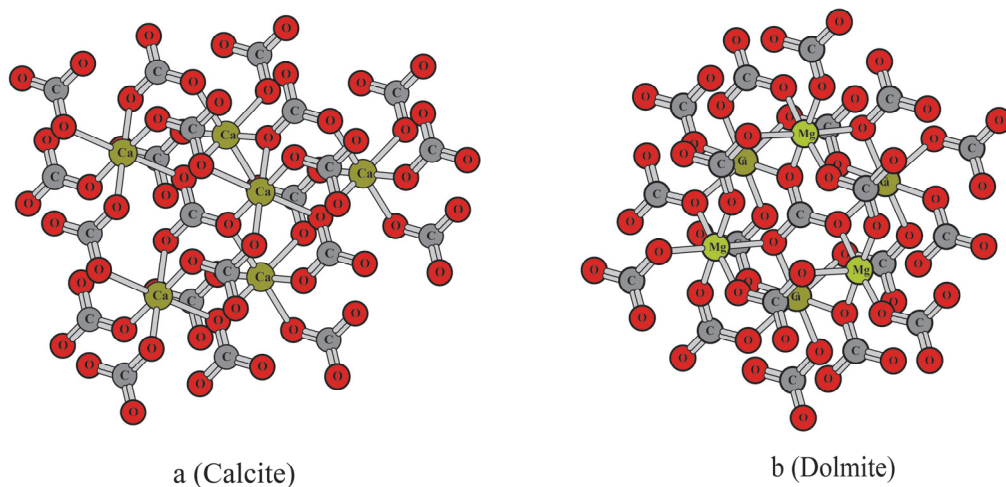


Figure 1. Structural diagram of calcite and dolomite. “a” depicts the schematic structure of calcite, while “b” represents the structure of dolomite.

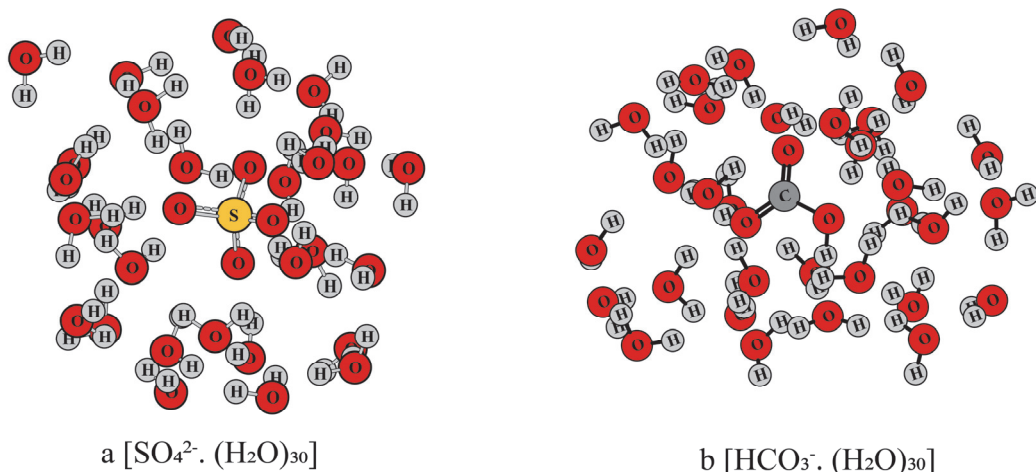


Figure 2. Structural diagram of $\text{SO}_4^{2-} \cdot (\text{H}_2\text{O})_{30}$ and $\text{HCO}_3^- \cdot (\text{H}_2\text{O})_{30}$. “a” depicts the schematic structure of $\text{SO}_4^{2-} \cdot (\text{H}_2\text{O})_{30}$, whereas “b” represents the structure of $\text{HCO}_3^- \cdot (\text{H}_2\text{O})_{30}$.

3. Results and Discussion

3.1 Isotope Fractionation Factors for Gas Systems

Researchers in geochemistry focus more on the isotope fractionation factors, α . Using the calculated $1000\ln\alpha$ values, we derived isotope fractionation factors ($1000\ln\alpha$) for H, O, S, and N in two phases under varying temperature conditions, employing two computational methods and comparing results to those of Richet et al. (1977) [8]. Table 1 and Figure. 3 present the $1000\ln\alpha$ values, showing that isotope fractionation factors are highest for hydrogen and lowest for sulfur. This indicates that elements with lower relative atomic mass are more likely to undergo isotope fractionation. Compared with Richet et al. (1977), the results from the B3LYP method align more closely. The B3LYP method showing better agreement than the HF method. The significant deviation in N_2O results may stem from simplifications in the thermodynamic modeling of molecular motion, or from errors introduced during early manual calculations, which were cumbersome and prone to inaccuracies. Familiarity with software like Quantum Espresso and Gaussian, and selecting the appropriate computational methods, will be essential for future research in isotope geochemistry and related fields.

Table 1. Comparison of $1000\ln\alpha$ values of H, O, S, and N calculated by two methods for different temperature conditions with Richet (1977) [8].

T (°C)	1000 $\ln\alpha$ [D/H (H ₂ -H ₂ O)]			1000 $\ln\alpha$ [³⁴ S/ ³² S (SO ₂ -H ₂ S)]			1000 $\ln\alpha$ [¹⁵ N/ ¹⁴ N (N ₂ O-NO)]			1000 α [¹⁸ O/ ¹⁶ O (CO ₂ -H ₂ O)]		
	B3LYP P	HF	Richet[8]	B3LYP P	HF	Richet[8]	B3LYP P	HF	Richet[8]	B3LYP P	HF	Richet[8]
0	1434. 846	1424. 553	1474.99 2	35.3	34.4	37.296	14.1	81.2	43.059	57.6 58	60.5 06	57.008
10	1373. 462	1363. 537	1412.20 6	33.4	32.4	35.367	13.3	77.9	40.182	54.4 16	57.1 63	53.796
20	1316. 140	1306. 710	1353.51 3	32.4	30.5	33.435	12.6	74.8	38.259	51.4 16	54.0 67	50.810
30	1262. 713	1253. 620	1299.10 1	30.5	29.5	31.499	12.0	71.9	36.332	48.6 34	51.1 94	48.064
T (°C)	1000 $\ln\alpha$ [D/H (H ₂ -H ₂ O)]			1000 $\ln\alpha$ [³⁴ S/ ³² S (SO ₂ -H ₂ S)]			1000 $\ln\alpha$ [¹⁵ N/ ¹⁴ N (N ₂ O-NO)]			1000 α [¹⁸ O/ ¹⁶ O (CO ₂ -H ₂ O)]		
	B3LYP P	HF	Richet[8]	B3LYP P	HF	Richet[8]	B3LYP P	HF	Richet[8]	B3LYP P	HF	Richet[8]
40	1212. 833	1203. 873	1247.89 4	28.5	27.6	30.529	11.4	69.2	35.367	46.0 49	48.5 23	45.469
50	1165. 959	1157. 196	1199.96 5	27.6	26.6	28.587	10.8	66.7	33.435	43.6 43	46.0 36	43.028
75	1060. 910	1052. 568	1092.25 9	24.6	23.7	25.668	9.63	61.0	29.559	38.3 09	40.5 16	37.754
100	970.0 21	962.0 29	999.160	21.7	20.7	22.739	8.60	56.0	26.642	33.7 92	35.8 33	33.211
125	890.7 68	882.9 41	918.289	18.8	18.8	20.783	7.73	51.6	24.693	29.9 37	31.8 29	29.433
150	821.1 01	813.5 93	846.726	17.8	16.8	18.822	6.99	47.8	21.761	26.6 24	28.3 82	26.163
175	759.4 03	751.8 88	783.445	15.8	14.8	16.857	6.36	44.3	19.803	23.7 60	25.3 96	23.322
200	704.0 87	697.1 39	727.549	13.9	13.9	14.889	5.80	41.3	18.822	21.2 72	22.7 97	20.830

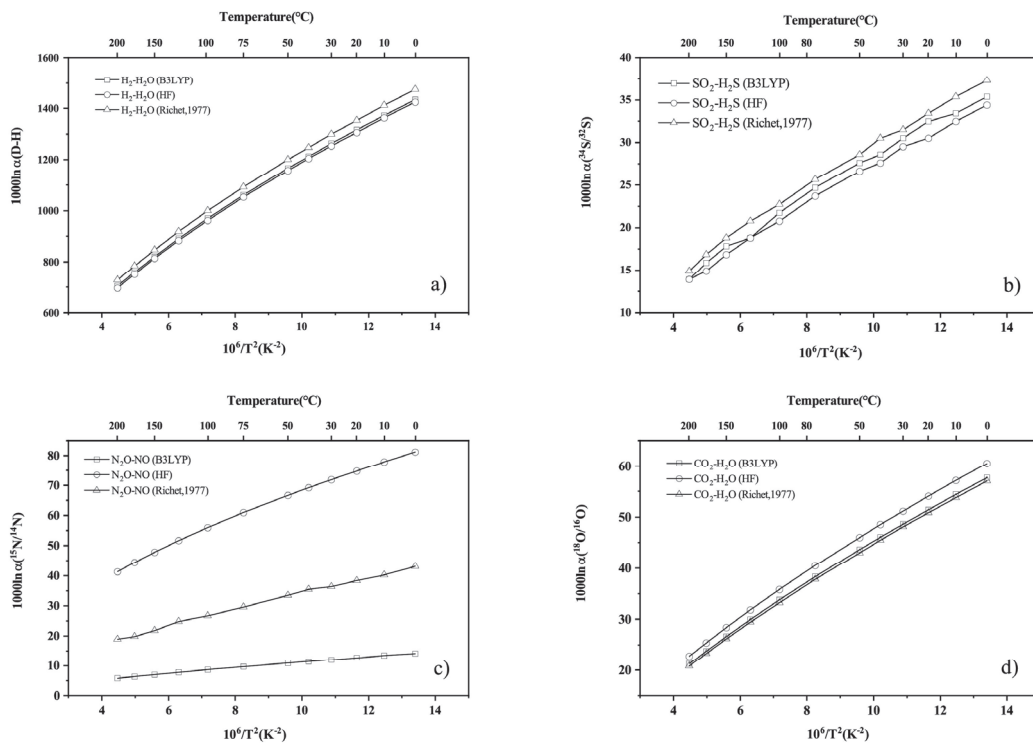


Figure 3. The plot of $1000\ln\alpha_{as}$ of H, O, S, and N was calculated by the two methods for different temperature conditions in comparison with Richet (1977). (a) hydrogen isotope fractionation between H_2 and H_2O , compared with the data from Richet (1977); (b) sulfur isotope fractionation between SO_2 and H_2S , also compared with Richet (1977); (c) nitrogen isotope fractionation between N_2O and NO , in comparison with Richet (1977); and (d) oxygen isotope fractionation between CO_2 and H_2O , compared with Richet (1977). The symbol “□” denotes B3LYP method calculations, “○” signifies HF method calculations, and “△” represents the results from Richet et al.

3.2 Isotope Fractionation Factors for Solution Systems

The oxygen isotope fractionation between sulfate and water has been extensively studied in previous research, with abundant data available from experimental studies [39-41], natural sample measurement [42-43] and theoretical calculations [44]. The study of carbonate solutions also provides valuable references for the computational results presented in this paper[45-47]. The calculated data in this paper were compared with the previous results (Table 2, Table 3, Figure. 4). The $1000\ln\alpha_{as}$ for $\text{SO}_4^{2-} \cdot (\text{H}_2\text{O})_{30}$ was calculated as 30.991 (‰) at 0°C using the B3LYP method, 23.197 (‰) using the HF method, and 33.043 (‰) based on the experimental data of Kusakabe and Robinson (1977) [41]. Relative to the HF method, the B3LYP method was significantly more accurate. In terms of polynomial fitting constants, the HF method produced values closer to those of Zeebe (2010)[44], as Zeebe also employed the HF method with a 6-31G (d, p) basis set. This basis set is consistent with the one used for the B3LYP calculations in this study. So, Zeebe (2010) is closer to the experimental value compared to the HF approach in this study. However, the HF method in this study yielded less accurate results compared to the B3LYP method, which may be attributed to the theoretical basis set selected for the HF approach being less high-level than that used for the B3LYP calculations. These findings highlight that the choice of computational method and theoretical basis set are critical factors influencing the accuracy of isotope fractionation calculations.

The values calculated for $\text{HCO}_3^- \cdot (\text{H}_2\text{O})_{30}$ show relatively large differences, with isotope fractionation factors decreasing as temperature increases. At 0°C, the differences among the methods are largest, but these differences decrease progressively with rising temperature. By 150°C, the B3LYP method results are generally in agreement with those of Beck et al. (2005)[45]. Below 150°C, the B3LYP values were higher than those from previous studies, while above 150°C, the B3LYP method calculated values became lower. Overall, the isotope fractionation

values calculated using the B3LYP method are closer to experimental data than those obtained using the HF method.

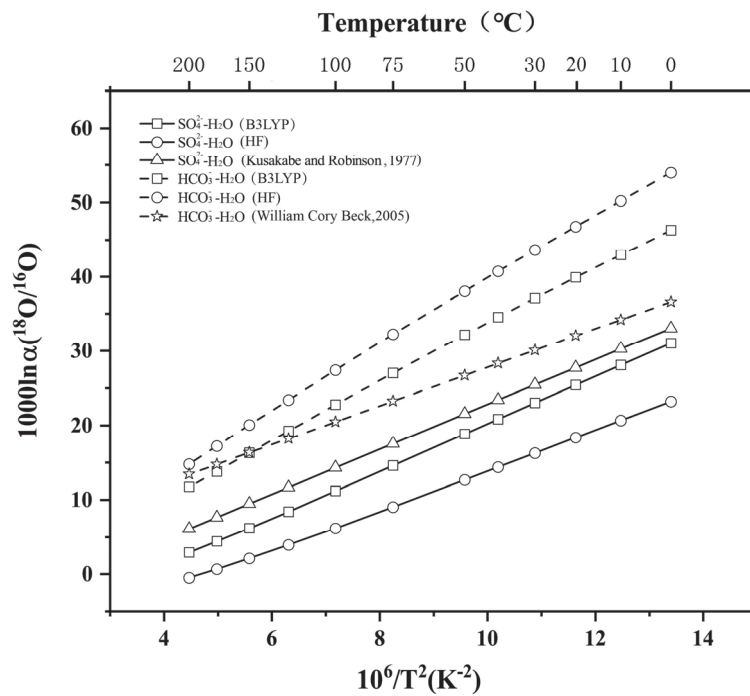


Figure 4. The plot of $1000\ln\alpha(^{18}\text{O}/^{16}\text{O})$ for the two calculation methods at different temperature conditions compared to experimental values. The straight line shows the calculation of $\text{SO}_4^{2-} \cdot (\text{H}_2\text{O})_{30}$, the dashed line shows the calculation of $\text{HCO}_3^- \cdot (\text{H}_2\text{O})_{30}$, “ \square ” shows the calculation of the B3LYP method, and “ \circ ” shows the calculation of the HF method. “ Δ ” indicates the experimental results of the study by Kusakabe, 1977, and “ \star ” indicates the results of Willam, 2005.

Table 2. $1000\ln\alpha$ values of $\text{SO}_4^{2-} \cdot (\text{H}_2\text{O})_{30}\text{-H}_2\text{O(g)}$ and $\text{HCO}_3^- \cdot (\text{H}_2\text{O})_{30}\text{-H}_2\text{O(g)}$ at different temperature conditions was calculated for two methods compared with previous studies.

T (°C)	$1000\ln\alpha [\text{SO}_4^{2-} \cdot (\text{H}_2\text{O})_{30}\text{-H}_2\text{O(g)}]$			$1000\ln\alpha [\text{HCO}_3^- \cdot (\text{H}_2\text{O})_{30}\text{-H}_2\text{O(g)}]$		
	B3LYP	HF	Kusakabe and Robinson [41].	B3LYP	HF	Beck et al [45].
0	30.991	23.197	33.043	46.308	53.982	36.603
10	28.071	20.654	30.243	42.97	50.231	34.195
20	25.424	18.358	27.726	39.915	46.794	32.028
30	23.021	16.281	25.453	37.113	43.639	30.073
40	20.835	14.401	23.395	34.539	40.737	28.302
50	18.844	12.695	21.524	32.17	38.063	26.692
75	14.594	9.081	17.533	27.018	32.236	23.258
100	11.19	6.221	14.317	22.774	27.424	20.491
125	8.446	3.944	11.688	19.252	23.418	18.228
150	6.221	2.125	9.51	16.308	20.059	16.355
175	4.411	0.668	7.687	13.832	17.225	14.786
200	2.931	-0.502	6.145	11.74	14.821	13.459

Table 3. Polynomial expansion of $1000\ln\alpha$ ($^{18}\text{O}/^{16}\text{O}$) for different solutions based on the function $1000\ln\alpha=ax+b$ with $x=10^3/T$ (T is the Kelvin temperature).

systems	Methods and references	Polynomial Expansion $1000\ln\alpha=ax+b$, $x=10^3/T$ (T is the Kelvin temperature)	
		a	b
SO_4^{2-} - $\text{H}_2\text{O(g)}$	B3LYP	3.159	-11.38
	HF	2.67	-12.76
	Kusakabe and Robinson[41].	3.01	-7.3
	Halas and Pluta[47].	2.41	-5.77
	Zeebe[44].	2.68	-7.45
HCO_3^- - $\text{H}_2\text{O(g)}$	B3LYP	3.884	-5.306
	HF	4.399	-4.418
	Beck et al[45].	2.59	1.890

3.3 Isotopic Fractionation Factors Between Minerals

In this section, calcite and dolomite were selected for structure optimization and frequency calculations. The initial crystal structures were obtained from the Crystal Database [37]. Mineral fragments were then constructed according to the modeling rules of the VVCM method. For calcite, the calculations revealed that the average bond length of the five central Ca-O bonds was 2.34Å using the HF method and 2.36Å using the B3LYP method, compared to the experimental value of 2.359Å [48]. For dolomite, the average bond lengths of the three Ca-O and three Mg-O bonds were 2.37Å and 2.06Å, respectively, using the HF method. 2.4Å and 2.1Å, respectively, using the B3LYP method. The experimental values for dolomite were 2.378Å for Ca-O and 2.081Å for Mg-O [49]. Refer to Table 4 for specific comparisons.

The calculated $1000\ln(\text{RPFR})$ values of calcite and dolomite were polynomially fitted, and the results were compared with the findings of Chacko[47] (Table S9). A comparison of the calculated oxygen isotope fractionation values ($1000\ln\alpha$) with those reported by Zheng [50] (Table 5, Table 6) showed the oxygen isotope fractionation values calculated for the two minerals are not significantly different. The results of the B3LYP method were closely aligned with Zheng's (1999) data, whereas the HF method showed significant deviations. Notably, the oxygen isotope fractionation factors for calcite-CO₂ at 0-10°C and dolomite-CO₂ at 0-20°C were negative when calculated using the HF method, but positive when calculated using the B3LYP method and Zheng's (1999) results. This discrepancy suggests that the HF method produces inconsistent results for heavy oxygen isotope enrichment at certain temperatures compared to the B3LYP method and Zheng's findings. Figure. 5 highlights the differences between the two calculation methods and their accuracy relative to previous studies, demonstrating that the B3LYP method yields results more consistent with experimental data.

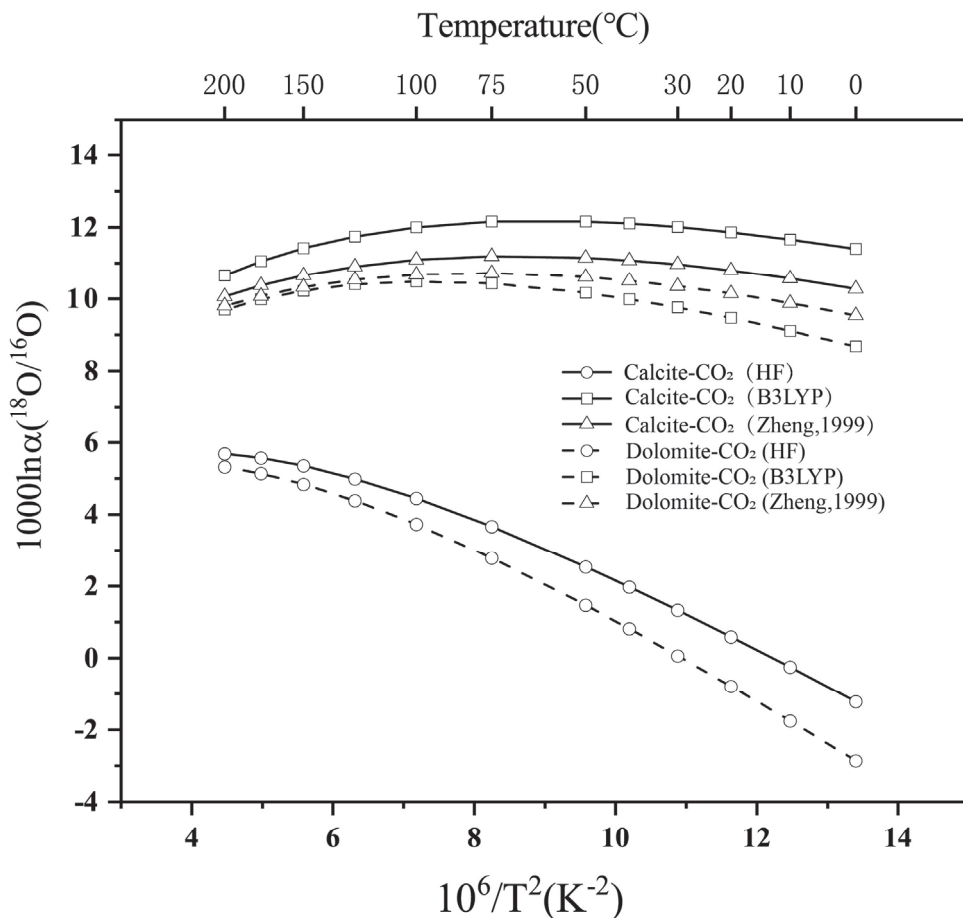


Figure 5. The plot of the $1000\ln\alpha_{\text{as}}$ of the two calculation methods compared with the results of previous studies. The solid lines indicate $1000\ln\alpha_{\text{as}}$ for calcite- $\text{CO}_2(\text{g})$, while the dotted lines represent the $1000\ln\alpha_{\text{as}}$ for dolomite- $\text{CO}_2(\text{g})$. The “□” symbolizes the B3LYP method calculation results, “○” denotes the HF method calculation outcomes, and “△” corresponds to the study of Zheng from 1999.

Table 4. Optimized bond lengths of calcite and dolomite structures compared to previous studies

Species	Methods and references	Bond lengths (\AA)	
		Ca-O	Mg-O
Calcite	B3LYP	2.36	/
	HF	2.34	/
	Zolotoyabko et al., 2010[49].	2.359	/
Dolomite	B3LYP	2.4	2.1
	HF	2.37	2.06
	Althoff, 1977[50].	2.378	2.081

Table 5. 1000lnα for systems calcite-CO₂ and dolomite-CO₂ compared to Zheng (1999)[51].

T (°C)	1000lnα[calcite-CO ₂ (g)]			1000lnα[dolomite-CO ₂ (g)]		
	B3LYP	HF	Zheng,1999	B3LYP	HF	Zheng,1999
0	11.394	-1.213	10.278	8.673	-2.859	9.534
10	11.660	-0.252	10.574	9.112	-1.757	9.879
20	11.862	0.590	10.798	9.472	-0.788	10.148
30	12.007	1.328	10.963	9.761	0.064	10.353
40	12.105	1.975	11.078	9.991	0.813	10.504
50	12.162	2.541	11.151	10.169	1.471	10.610
75	12.160	3.662	11.194	10.428	2.786	10.724
100	12.005	4.451	11.095	10.487	3.727	10.682
125	11.746	4.993	10.904	10.406	4.389	10.539
150	11.419	5.350	10.656	10.228	4.844	10.329
175	11.049	5.570	10.372	9.984	5.141	10.078
200	10.654	5.686	10.068	9.696	5.321	9.802

Table 6. 1000lnα polynomial constants for oxygen isotopes in calcite and dolomite with carbon dioxide

1000lnα	Methods and references	1000lnα polynomial constants for oxygen isotopes in calcite and dolomite with carbon dioxide $1000\ln\alpha = C_1 \cdot x^2 + C_2 \cdot x + C_3$ $x = 10^3/T$ (T is the Kelvin temperature)		
		C ₁	C ₂	C ₃
1000α(c -cal)	HF	-2.261	8.552	-2.254
	B3LYP	-1.903	11.44	-4.994
	Zheng1999[51]].	-1.71	10.01	-3.45
1000α(c -dol)	HF	-2.456	8.85	-2.374
	B3LYP	-2.055	11.17	-4.712
	Zheng1999[51]].	-1.76	9.99	-3.45

4. Conclusion

The rapid development of isotope theoretical calculations, supported by advancements in computational technology, has significantly simplified research processes while improving calculation accuracy compared to earlier methods. Different computational approaches and software have enhanced the efficiency of isotope geochemistry research. In this study, first-principles theoretical calculations were employed to investigate isotope fractionation effects across gas, liquid, and solid systems. The key conclusions are as follows: (1) Elements with lighter atomic masses undergo greater isotope fractionation compared to heavier elements. (2) The isotope fractionation factors are temperature-dependent: as temperature increases, the isotope fractionation factors decrease. This is the reason that theoretical computations can assist us in resolving issues resulting from experimental conditions that are unachievable in reality. (3) Comparative analysis of the B3LYP and HF calculation methods demonstrates that data obtained using the B3LYP method align more closely with previous research, indicating that the B3LYP approach is more accurate. This is why many researchers prefer the B3LYP method for their calculations. The employment of different theoretical basis sets will influence the outcomes of the calculation, and the higher the theoretical basis sets, the more accurate the calculation results will be. The findings of this study provide a useful reference for future researchers in selecting appropriate computational methods. Additionally, the data presented in this paper can offer theoretical support for understanding geochemical processes and isotope studies of simple elements.

Acknowledgments

This work has been financially supported by Chinese National Science Fund Projects. The authors also thank the financial support from the Science and Technology Program of Guizhou. We also appreciate the experimental convenience provided by Guizhou Normal University/State Engineering Technology Institute for Karst Desertification. We would also like to thank ChatGPT for its assistance in translating.

References

- [1] Ye, H., Wu, C., Brzozowski, M. J., et al. (2020). Calibrating equilibrium Fe isotope fractionation factors between magnetite, garnet, amphibole, and biotite. *Geochimica et Cosmochimica Acta*, 271, 78–95. <https://doi.org/10.1016/j.gca.2019.12.004>
- [2] Schauble, E. A. (2004). Applying stable isotope fractionation theory to new systems. *Reviews in Mineralogy and Geochemistry*, 55(1), 65–111. <https://doi.org/10.2138/gsrmg.55.1.65>
- [3] Young, E. D., Manning, C. E., Schauble, E. A., et al. (2015). High-temperature equilibrium isotope fractionation of non-traditional stable isotopes: Experiments, theory, and applications. *Chemical Geology*, 395, 176–195. <https://doi.org/10.1016/j.chemgeo.2014.12.013>
- [4] Lindemann, F. A., & Aston, F. W. (1919). XLVIII. The possibility of separating isotopes. *The London, Edinburgh, and Dublin Philosophical Magazine and Journal of Science*, 37(221), 523–534. <https://doi.org/10.1080/14786440508635914>
- [5] Urey, H. C., & Greiff, L. J. (1935). Isotopic exchange equilibria. *Journal of the American Chemical Society*, 57(2), 321–327. <https://doi.org/10.1021/ja01305a021>
- [6] Urey, H. C. (1947). The thermodynamic properties of isotopic substances. *Journal of the Chemical Society (Resumed)*, 562–581. <https://doi.org/10.1039/JR9470000562>
- [7] Bigeleisen, J., & Mayer, M. G. (1947). Calculation of equilibrium constants for isotopic exchange reactions. *The Journal of Chemical Physics*, 15(5), 261–267. <https://doi.org/10.1063/1.1746492>
- [8] Richet, P., Bottinga, Y., & Javoy, M. (1977). A review of hydrogen, carbon, nitrogen, oxygen, sulphur, and chlorine stable isotope fractionation among gaseous molecules. *Annual Review of Earth and Planetary Sciences*, 5(1), 65–110. <https://doi.org/10.1146/annurev.ea.05.050177.000433>
- [9] Adnew, G. A., Workman, E., Janssen, C., et al. (2022). Temperature dependence of isotopic fractionation in the CO₂-O₂ isotope exchange reaction. *Rapid Communications in Mass Spectrometry*, 36(12), e9301. <https://doi.org/10.1002/rcm.9301>
- [10] Bigeleisen, J. (1961). Statistical mechanics of isotope effects on the thermodynamic properties of condensed systems. *The Journal of Chemical Physics*, 34(5), 1485–1493. <https://doi.org/10.1063/1.1701034>
- [11] Jakli, G., Chan, T. C., & Van Hook, W. A. (1975). Equilibrium isotope effects in aqueous systems. IV. The vapor pressures of NaBr, NaI, KF, Na₂SO₄, and CaCl₂ solutions in H₂O and D₂O (0 to 90°C). Vapor pressures of Na₂SO₄·10H₂O, ·10D₂O and CaCl₂·2H₂O, ·2D₂O. *Journal of Solution Chemistry*, 4(1), 71–90. <https://doi.org/10.1007/BF00649751>
- [12] Bottinga, Y. (1968). Calculation of fractionation factors for carbon and oxygen isotopic exchange in the system calcite-carbon dioxide-water. *The Journal of Physical Chemistry*, 72(3), 800–808. <https://doi.org/10.1021/j100849a008>
- [13] Zheng, Y.-F. (1991). Calculation of oxygen isotope fractionation in metal oxides. *Geochimica et Cosmochimica Acta*, 55(8), 2299–2307. [https://doi.org/10.1016/0016-7037\(91\)90105-W](https://doi.org/10.1016/0016-7037(91)90105-W)
- [14] Xiao, Z. C., Zhou, C., Kang, J. T., et al. (2022). The factors controlling equilibrium inter-mineral Ca isotope fractionation: Insights from first-principles calculations. *Geochimica et Cosmochimica Acta*, 333, 373–389. <https://doi.org/10.1016/j.gca.2022.07.013>
- [15] Ferrari, C., Méheut, M., Resongles, E., et al. (2022). Equilibrium mass-dependent isotope fractionation of antimony between stibnite and Sb secondary minerals: A first-principles study. *Chemical Geology*, 611, 121115. <https://doi.org/10.1016/j.chemgeo.2022.121115>
- [16] Duan, H., Yang, B., & Huang, F. (2023). Site-specific isotope effect: Insights from equilibrium magnesium isotope fractionation in mantle minerals. *Geochimica et Cosmochimica Acta*, 357, 13–25. <https://doi.org/10.1016/j.gca.2023.07.008>
- [17] Criss, R. E. (1999). *Principles of stable isotope distribution*. Oxford University Press.

- [18] Yang, J., Li, Y., Liu, S., et al. (2015). Theoretical calculations of Cd isotope fractionation in hydrothermal fluids. *Chemical Geology*, 391, 74–82. <https://doi.org/10.1016/j.chemgeo.2014.10.028>
- [19] Young, E. D., Manning, C. E., Schauble, E. A., et al. (2015). High-temperature equilibrium isotope fractionation of non-traditional stable isotopes: Experiments, theory, and applications. *Chemical Geology*, 395, 176–195. <https://doi.org/10.1016/j.chemgeo.2014.12.013>
- [20] Zhao, Y., Li, Y., Wiggenhauser, M., et al. (2021). Theoretical isotope fractionation of cadmium during complexation with organic ligands. *Chemical Geology*, 571, 120178. <https://doi.org/10.1016/j.chemgeo.2021.120178>
- [21] Ratié, G., Chrastný, V., Guinoiseau, D., et al. (2021). Cadmium isotope fractionation during complexation with humic acid. *Environmental Science & Technology*, 55(11), 7430–7444. <https://doi.org/10.1021/acs.est.0c07824>
- [22] Yamaji, K., Makita, Y., Watanabe, H., et al. (2001). Theoretical estimation of lithium isotopic reduced partition function ratio for lithium ions in aqueous solution. *The Journal of Physical Chemistry A*, 105(3), 602–613. <https://doi.org/10.1021/jp002868q>
- [23] Schauble, E. A., Méheut, M., & Hill, P. S. (2009). Combining metal stable isotope fractionation theory with experiments. *Elements*, 5(6), 369–374. <https://doi.org/10.2113/gselements.5.6.369>
- [24] Mavromatis, V., Gautier, Q., Bosc, O., et al. (2013). Kinetics of Mg partition and Mg stable isotope fractionation during its incorporation in calcite. *Geochimica et Cosmochimica Acta*, 114, 188–203. <https://doi.org/10.1016/j.gca.2013.03.024>
- [25] Brazier, J. M., Blanchard, M., Méheut, M., et al. (2023). Experimental and theoretical investigations of stable Sr isotope fractionation during its incorporation in aragonite. *Geochimica et Cosmochimica Acta*, 358, 134–147. <https://doi.org/10.1016/j.gca.2023.08.011>
- [26] Fujii, T., Kato, C., Wada, N., et al. (2023). Theoretical and experimental study on vanadium isotope fractionation among species relevant to geochemistry. *ACS Earth and Space Chemistry*, 7(4), 912–925. <https://doi.org/10.1021/acsearthspacechem.2c00387>
- [27] Bartlett, R. J. (Ed.). (1997). *Recent advances in coupled-cluster methods*. World Scientific Publishing.
- [28] Del Bene, J. E. (Ed.). (2002). *Recent advances in density functional methods*. World Scientific Publishing.
- [29] Koch, W., & Holthausen, M. C. (2015). *A chemist's guide to density functional theory* (2nd ed.). Wiley-VCH.
- [30] Giannozzi, P., Baroni, S., Bonini, N., et al. (2009). QUANTUM ESPRESSO: A modular and open-source software project for quantum simulations of materials. *Journal of Physics: Condensed Matter*, 21(39), 395502. <https://doi.org/10.1088/0953-8984/21/39/395502>
- [31] Giannozzi, P., Andreussi, O., Brumme, T., et al. (2017). Advanced capabilities for materials modelling with Quantum ESPRESSO. *Journal of Physics: Condensed Matter*, 29(46), 465901. <https://doi.org/10.1088/1361-648X/aa8f79>
- [32] Frisch, M. J. (2004). *Gaussian 03, Revision E.01* [Computer software]. Gaussian, Inc. <http://www.gaussian.com/>
- [33] Gao, T., Gillispie, G. J., Copus, J. S., et al. (2018). Optimization of gelatin-alginate composite bioink printability using rheological parameters: A systematic approach. *Biofabrication*, 10(3), 034106. <https://doi.org/10.1088/1758-5090/aacd7>
- [34] He, C., Liu, L., Chu, Y., et al. (2017). National and subnational all-cause and cause-specific child mortality in China, 1996–2015: A systematic analysis with implications for the Sustainable Development Goals. *The Lancet Global Health*, 5(2), e186–e197. [https://doi.org/10.1016/S2214-109X\(16\)30334-2](https://doi.org/10.1016/S2214-109X(16)30334-2)
- [35] Zhang, J. (2021). Equilibrium sulfur isotope fractionations of several important sulfides. *Geochemical Journal*, 55(3), 135–147. <https://doi.org/10.2343/geochemj.2.0620>
- [36] Zhang, Y., & Liu, Y. (2018). The theory of equilibrium isotope fractionations for gaseous molecules under super-cold conditions. *Geochimica et Cosmochimica Acta*, 238, 123–149. <https://doi.org/10.1016/j.gca.2018.07.002>
- [37] Graf, D. L. (1961). Crystallographic tables for the rhombohedral carbonates. *American Mineralogist: Journal of Earth and Planetary Materials*, 46(11-12), 1283–1316.
- [38] Liu, Y., & Tossell, J. A. (2005). Ab initio molecular orbital calculations for boron isotope fractionations on

- boric acids and borates. *Geochimica et Cosmochimica Acta*, 69(16), 3995–4006. <https://doi.org/10.1016/j.gca.2005.04.008>
- [39] Cortecchi, G. (1974). Oxygen isotopic ratios of sulfate ions-water pairs as a possible geothermometer. *Geothermics*, 3(2), 60–64. [https://doi.org/10.1016/0375-6505\(74\)90014-9](https://doi.org/10.1016/0375-6505(74)90014-9)
- [40] Lloyd, R. M. (1968). Oxygen isotope behavior in the sulfate-water system. *Journal of Geophysical Research*, 73(18), 6099–6110. <https://doi.org/10.1029/JB073i018p06099>
- [41] Kusakabe, M., & Robinson, B. W. (1977). Oxygen and sulfur isotope equilibria in the BaSO₄-HSO₄-H₂O system from 110 to 350°C and applications. *Geochimica et Cosmochimica Acta*, 41(8), 1033–1040. [https://doi.org/10.1016/0016-7037\(77\)90192-9](https://doi.org/10.1016/0016-7037(77)90192-9)
- [42] Boschetti, T. (2013). Oxygen isotope equilibrium in sulfate–water systems: A revision of geothermometric applications in low-enthalpy systems. *Journal of Geochemical Exploration*, 124, 92–100. <https://doi.org/10.1016/j.gexplo.2012.08.013>
- [43] Chiba, H., & Sakai, H. (1985). Oxygen isotope exchange rate between dissolved sulfate and water at hydrothermal temperatures. *Geochimica et Cosmochimica Acta*, 49(4), 993–1000. [https://doi.org/10.1016/0016-7037\(85\)90317-1](https://doi.org/10.1016/0016-7037(85)90317-1)
- [44] Zeebe, R. E. (2010). A new value for the stable oxygen isotope fractionation between dissolved sulfate ion and water. *Geochimica et Cosmochimica Acta*, 74(3), 818–828. <https://doi.org/10.1016/j.gca.2009.10.033>
- [45] Beck, W. C., Grossman, E. L., & Morse, J. W. (2005). Experimental studies of oxygen isotope fractionation in the carbonic acid system at 15, 25, and 40 °C. *Geochimica et Cosmochimica Acta*, 69(14), 3493–3503. <https://doi.org/10.1016/j.gca.2005.02.003>
- [46] Pathak, A. K., Mukherjee, T., & Maity, D. K. (2008). Theoretical study on the spectroscopic properties of CO₃–nH₂O clusters: Extrapolation to bulk. *ChemPhysChem*, 9(15), 2259–2264. <https://doi.org/10.1002/cphc.200800350>
- [47] Chacko, T., & Deines, P. (2008). Theoretical calculation of oxygen isotope fractionation factors in carbonate systems. *Geochimica et Cosmochimica Acta*, 72(15), 3642–3660. <https://doi.org/10.1016/j.gca.2008.06.001>
- [48] Zolotoyabko, E., Caspi, E. N., Fieramosca, J. S., et al. (2010). Differences between bond lengths in biogenic and geological calcite. *Crystal Growth & Design*, 10(3), 1207–1214. <https://doi.org/10.1021/cg901177h>
- [49] Althoff, P. L. (1977). Structural refinements of dolomite and a magnesian calcite and implications for dolomite formation in the marine environment. *American Mineralogist*, 62(7-8), 772–783.
- [50] Zheng, Y.-F. (1999). Oxygen isotope fractionation in carbonate and sulfate minerals. *Geochemical Journal*, 33(2), 109–126. <https://doi.org/10.2343/geochemj.33.109>

Copyrights

Copyright for this article is retained by the author(s), with first publication rights granted to the journal.

This is an open-access article distributed under the terms and conditions of the Creative Commons Attribution license (<http://creativecommons.org/licenses/by/4.0/>).